Stem Cell Reports
Article

ISSCR

OPEN ACCESS

Activation of IRF1 in Human Adipocytes Leads to Phenotypes Associated with Metabolic Disease

Max Friesen,[1,4,12] Raymond Camahort,[1,2,3,12] Youn-Kyoung Lee,[1,12] Fang Xia,[1] Robert E. Gerszten,[5,6] Eugene P. Rhee,[6,7] Rahul C. Deo,[8,9,10,11] and Chad A. Cowan[1,2,3,*]

[1]Department of Stem Cell and Regenerative Biology, Harvard University, Cambridge, MA 02138, USA
[2]Center for Regenerative Medicine, Massachusetts General Hospital, Boston, MA 02114, USA
[3]Harvard Stem Cell Institute, Harvard University, Cambridge, MA 02138, USA
[4]Department of Anatomy and Embryology, Leiden University Medical Center, 2333 ZA Leiden, the Netherlands
[5]Cardiovascular Research Center, Massachusetts General Hospital, Harvard Medical School, Boston, MA 02114, USA
[6]Broad Institute of MIT and Harvard, Cambridge, MA 02142, USA
[7]Nephrology Division, Massachusetts General Hospital, Harvard Medical School, Boston, MA 02114, USA
[8]Department of Medicine
[9]Institute for Human Genetics
University of California San Francisco, San Francisco, CA 94143, USA
[10]California Institute for Quantitative Biosciences, San Francisco, CA 94158, USA
[11]Cardiovascular Research Institute, University of California San Francisco, San Francisco, CA 94143, USA
[12]Co-first author
*Correspondence: chadacowan@gmail.com
http://dx.doi.org/10.1016/j.stemcr.2017.03.014

SUMMARY

The striking rise of obesity-related metabolic disorders has focused attention on adipocytes as critical mediators of disease phenotypes. To better understand the role played by excess adipose in metabolic dysfunction it is crucial to decipher the transcriptional underpinnings of the low-grade adipose inflammation characteristic of diseases such as type 2 diabetes. Through employing a comparative transcriptomics approach, we identified *IRF1* as differentially regulated between primary and in vitro-derived genetically matched adipocytes. This suggests a role as a mediator of adipocyte inflammatory phenotypes, similar to its function in other tissues. Utilizing adipose-derived mesenchymal progenitors we subsequently demonstrated that expression of *IRF1* in adipocytes indeed contributes to upregulation of inflammatory processes, both in vitro and in vivo. This highlights *IRF1*'s relevance to obesity-related inflammation and the resultant metabolic dysregulation.

INTRODUCTION

Obesity is a disease in which the energy reserve stored in the adipose tissue has increased excessively to cause adverse health effects. Adipocytes play a critical role in the regulation of triglyceride storage, glucose homeostasis, and energy expenditure. Excess adipose can disrupt this regulation. Obesity-related metabolic diseases, including type 2 diabetes mellitus (T2DM), have reached epidemic proportions and have been recognized as a leading contributor to morbidity and premature mortality (Ogden et al., 2012). More than 85% of people diagnosed with T2DM are overweight or obese (ADA, 2012).

Adipocyte biology has garnered increased attention because of this. Chronic low-grade inflammation of adipose tissue has emerged as an important contributor to obesity-induced insulin resistance (Gregor and Hotamisligil, 2011). Inflammation of adipose tissue is thought to occur due to nutrient overload in adipocytes, activating inflammatory pathways and leading to the recruitment of immune cells. In the context of obesity, adipocytes are a critical source of inflammatory chemokines that contribute to metabolic disease.

Transcriptional profiling of adipocytes has identified several regulators of adipogenesis (transcription factors, long non-coding RNAs, and microRNAs) (Urs et al., 2004). Unfortunately, few transcriptional regulators of adipose inflammation have been identified due to the in vitro nature of these studies. Therefore, the mechanistic underpinnings of how adipocytes contribute to metabolic diseases such as T2DM are underappreciated. To identify determinants of adipose inflammation, we transcriptionally profiled primary human adipocytes isolated from obese donors. We then compared expression data with in vitro-derived adipocytes. By focusing on differentially regulated transcription factors with a known function in immune response, we prioritized interferon regulatory factor 1 (IRF1). Subsequently we examined its role in adipose inflammation.

RESULTS

Comparative Expression Analysis of Primary versus In Vitro-Derived Adipocytes

For expression analysis of primary and in vitro-derived adipocytes, we obtained whole subcutaneous adipose tissue from two obese females (body mass index >30; 41 and 59 years old) undergoing elective abdominoplasty. Primary adipocytes were isolated from whole adipose tissue. We

verified the integrity of the adipocytes using fluorescence microscopy, showing the large unilocular lipid droplet typical of white adipocytes (Figure 1A). In addition, we isolated adipose stromovascular cells (ASCs) from one of the donors (59 years). The ASCs were subsequently differentiated into adipocytes at >90% efficiency (Figures 1B and S1A), and adipocyte-specific gene expression was measured (Figure S1B).

RNA was extracted from the above cell types and subjected to whole-genome microarray analysis. Hierarchical clustering accurately grouped replicates of adipocytes, ASCs, and ASC adipocytes, with significant expression differences between groups (Figure 1C). We identified 1,749 genes with >1.7-fold higher abundance in primary adipocytes versus ASC adipocytes at a 0.1% false discovery rate (FDR) (Table S1). Gene ontology enrichment analysis for the primary adipocyte-enriched genes was consistent with a phenotype of inflammation, with enriched terms including "response to type I interferon," "immune response," and "positive regulation of chemotaxis" (Table S2). Genes with increased expression in the aforementioned pathways reflect a spectrum of inflammatory mediators, including interferon-regulated transcription factors (*IRF1*, *IRF8*), chemokines (*CCL2/MCP1*, *CCL8*), cytokines (*IL6*, *IL8*), Toll-like receptors (*TLR1*, *TLR3*), and inflammasome components (*NLRP3*). This inflammatory signature was not observed in undifferentiated ASCs either.

To control for contribution of stromovascular fraction cells (SVFs) to the inflammatory expression signature we isolated the SVF pellet, as contaminating immune cell transcripts should be identified in this fraction as well. Of the 1,749 transcripts identified to be specifically upregulated in primary adipocytes compared with ASC adipocytes, 1,009 were more abundant in the primary adipocytes compared with the SVFs, providing a conservative estimate for the fraction of genes with an adipocyte origin (Table S3). This list of 1,009 genes includes all of the inflammatory mediators listed above. The highest expressed immunoregulatory transcription factor in primary compared with ASC adipocytes was IRF1 (14.3-fold, $p = 7.50 \times 10^{-23}$). We sought to validate this result in two additional datasets. Comparing four additional primary adipocyte samples with three unmatched ASC adipocytes, we found a 33-fold upregulation of *IRF1* in the primary adipocytes (Figure 1D). To ascertain that increased *IRF1* expression is specific to obesity, we analyzed a publicly available dataset (GEO dataset GDS3602) comparing primary adipocytes from ten lean versus ten obese individuals, and found a 3.72-fold increase in *IRF1* expression in adipocytes from obese individuals (Figure 1E; Lee et al., 2005). A large portion of genes overexpressed in obese individuals from this dataset (1.7-fold, 0.1% FDR) (Table S4) overlaps with genes we found upregulated in primary adipocytes (Figure S1C). The list of overlapping genes includes, but is not limited to, inflammatory genes such as the aforementioned *IRF1*, *CCL2*, *CCL8*, *IL6*, and *IL8* (Table S5).

Expression of IRF1 in Adipocytes Activates the Immune Response

Utilizing lentivirus to express a doxycycline-inducible transgene, we devised a scheme to express *IRF1* in ASC adipocytes (IRF1 adipocytes) (Figure 2A). After several days of doxycycline treatment we confirmed the expression of ectopic IRF1 (Figure S2A). Chromatin immunoprecipitation qPCR (ChIP-qPCR) revealed that ectopic IRF1 binds near genes that contain an IRF1-binding motif proximal to their promoter (*PARP14*, *IFIT3*, *ISG15*), and IRF1 binding correlates with increased expression of these genes (Figure 2B). There is no expression difference or IRF1 binding in genes without this motif (*OAS3*, *ZNF74*). When *IRF1* is not overexpressed, we do not see this effect (Figure S2B). In differentiated adipocytes, *IRF1* overexpression affected the mRNA levels of relatively few genes (138 upregulated, 80 downregulated, 1.7-fold, 0.1% FDR) (Figure 2C and Table S5). The majority of upregulated genes in IRF1 adipocytes are associated with innate immunity, including major histocompatibility complex (MHC) class I receptors, interferon-responsive genes, and chemotactic cytokines. Immune response-associated genes found to be upregulated in IRF1 adipocytes are also increased in primary adipocytes compared with ASC adipocytes. Furthermore, 103 of the 138 differentially regulated genes were previously reported as known interferon-responsive genes, confirming that we are observing a bona fide interferon-like response in IRF1 adipocytes (Samarajiwa et al., 2009). This leads us to conclude that ASC adipocytes expressing IRF1 more closely resemble primary human obese adipocytes.

IRF1 Alters Metabolism and Lipid Droplet Composition of Adipocytes In Vitro

Experimental evidence shows that the interferon response pathway associates with altered adipocyte metabolism, as treatment of in vitro-derived adipocytes with interferon-γ induces insulin resistance (McGillicuddy et al., 2009). The known role of *IRF1* in the interferon response and the upregulation of inflammatory genes in IRF adipocytes led us to hypothesize that *IRF1* contributes to adipose inflammation. To further characterize *IRF1* activation, we performed a multiplex ELISA to determine levels of cytokines and adipokines released by IRF1 adipocytes (Figures 3A and S2C). We found secretion of pro-inflammatory cytokines interleukin-6 (IL-6) and IL-8, as well as monocyte chemotactic protein 1 (MCP-1), were significantly elevated in IRF1 adipocytes concomitant with the increase in RNA. We also found these genes to be upregulated in obese individuals (Figure S2D).

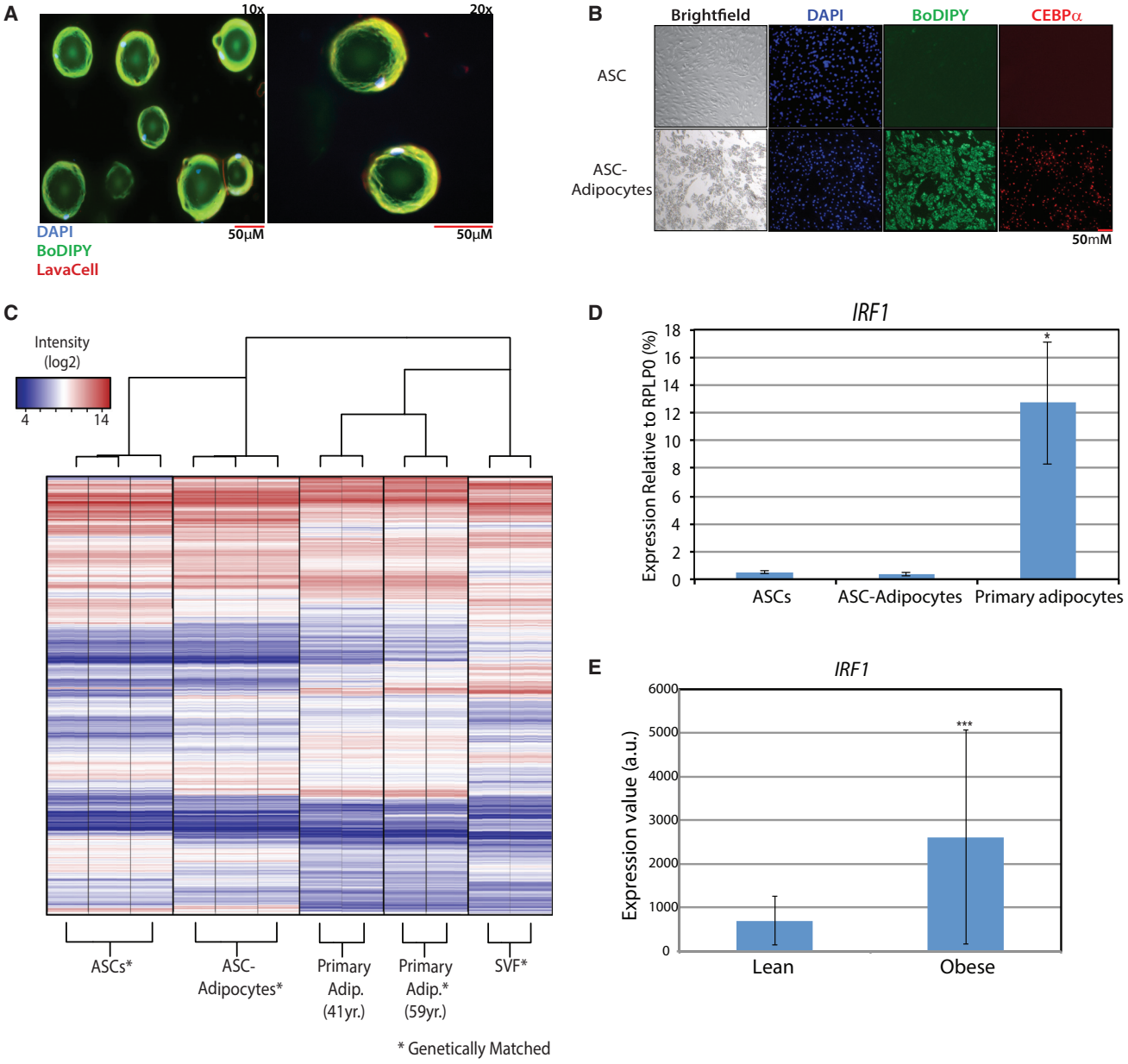

Figure 1. Primary and ASC-Adipocyte Integrity and Transcriptional Profiling

(A) Primary adipocytes isolated from whole adipose. Adipocytes were stained with DAPI to visualize the DNA (blue), BoDIPY to stain the lipid droplet (green), and LavaCell to stain the plasma membrane (red), and visualized by wide-field microscopy.

(B) ASCs were differentiated into adipocytes and stained with DAPI to visualize the DNA (blue), BoDIPY to stain lipids (green), and an antibody to visualize C/EBPα (red).

(C) Hierarchical clustering and heatmap representation of transcriptional profiles (mRNA) from ASCs, ASC adipocytes, and primary adipocytes. Probe sets are colored according to expression level.

(D) Gene expression of IRF1 in ASCs (n = 3), ASC adipocytes (n = 3), and primary adipocytes (n = 4).

(E) Gene expression of IRF1 in isolated subcutaneous adipocytes of lean (n = 10) and obese (n = 10) individuals.

For all graphs, error bars represent SD, experiments were performed in biological triplicates and statistically significant p values are denoted by asterisks (*$p \leq 0.05$, **$p \leq 0.005$).

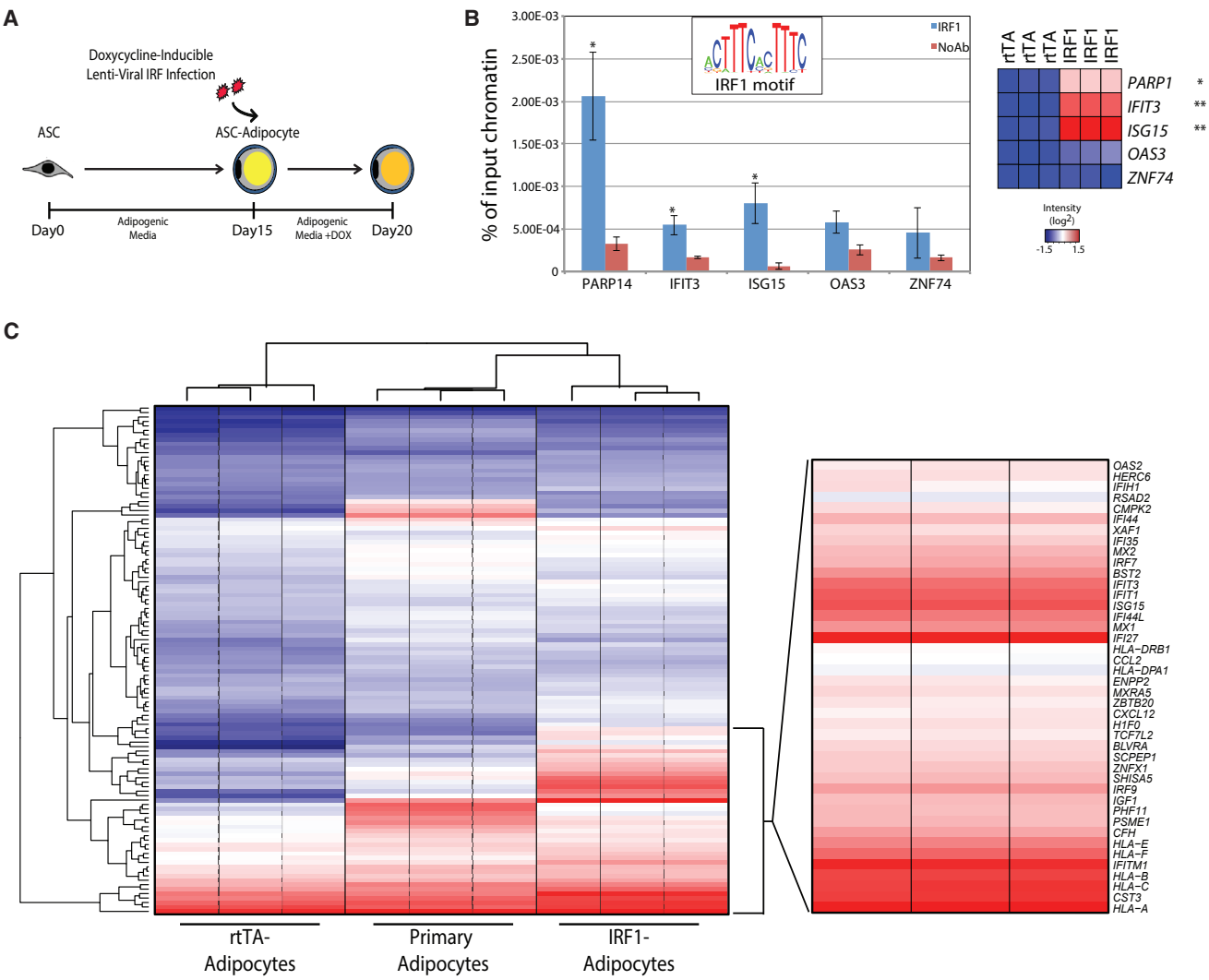

Figure 2. IRF1 Expression Leads to an Inflammatory Gene Signature

(A) Experimental scheme to ectopically express IRF1 in mature ASC adipocytes.

(B) ChIP-qPCR (n = 3) was performed for IRF1 at putative binding sites (H3K4me1 bound IRF1 motif) (*PARP14*, *IFIT3*, *ISG15*). *OAS3* and *ZNF74* represent a negative control site where IRF1 is not predicted to bind. Signals are expressed as percentage of total chromatin input. The heatmap represents expression levels of these genes in IRF1 and rtTA adipocytes.

(C) Hierarchical clustering and heatmap representation of transcriptional profiles (mRNA) from rtTA adipocytes, IRF1 adipocytes, and primary adipocytes. Probe sets are colored according to expression level. The highest expressed 30% of genes in IRF-1 adipocytes have been expanded to highlight their inflammatory nature.

Error bars represent SD, experiments were performed in biological triplicates, and statistically significant p values are denoted by asterisks ($*p \leq 0.05$, $**p \leq 0.005$).

Since obese adipocytes display reduced lipolysis in vivo, we performed a lipolysis assay to measure the ability of IRF1 adipocytes to catabolize intracellular lipids. In response to β-adrenergic stimulation, IRF1 adipocytes were unable to increase triglyceride hydrolysis, unlike control cells (Figures 3B and S2E). To assess insulin sensitivity, we performed a glucose uptake assay. Expression of *IRF1* abrogates insulin-mediated glucose uptake in ASC adipocytes, consistent with the increase in pro-inflammatory signaling and altered lipid metabolism (Figure 3C).

Unlike their in vivo counterparts, in vitro-derived adipocytes typically display multilocular lipid droplets. After several days of *IRF1* expression, ASC adipocytes demonstrate a transition from a multilocular to unilocular state and the average size of the largest lipid droplet increases significantly (Figure 3D). The total intracellular triglyceride

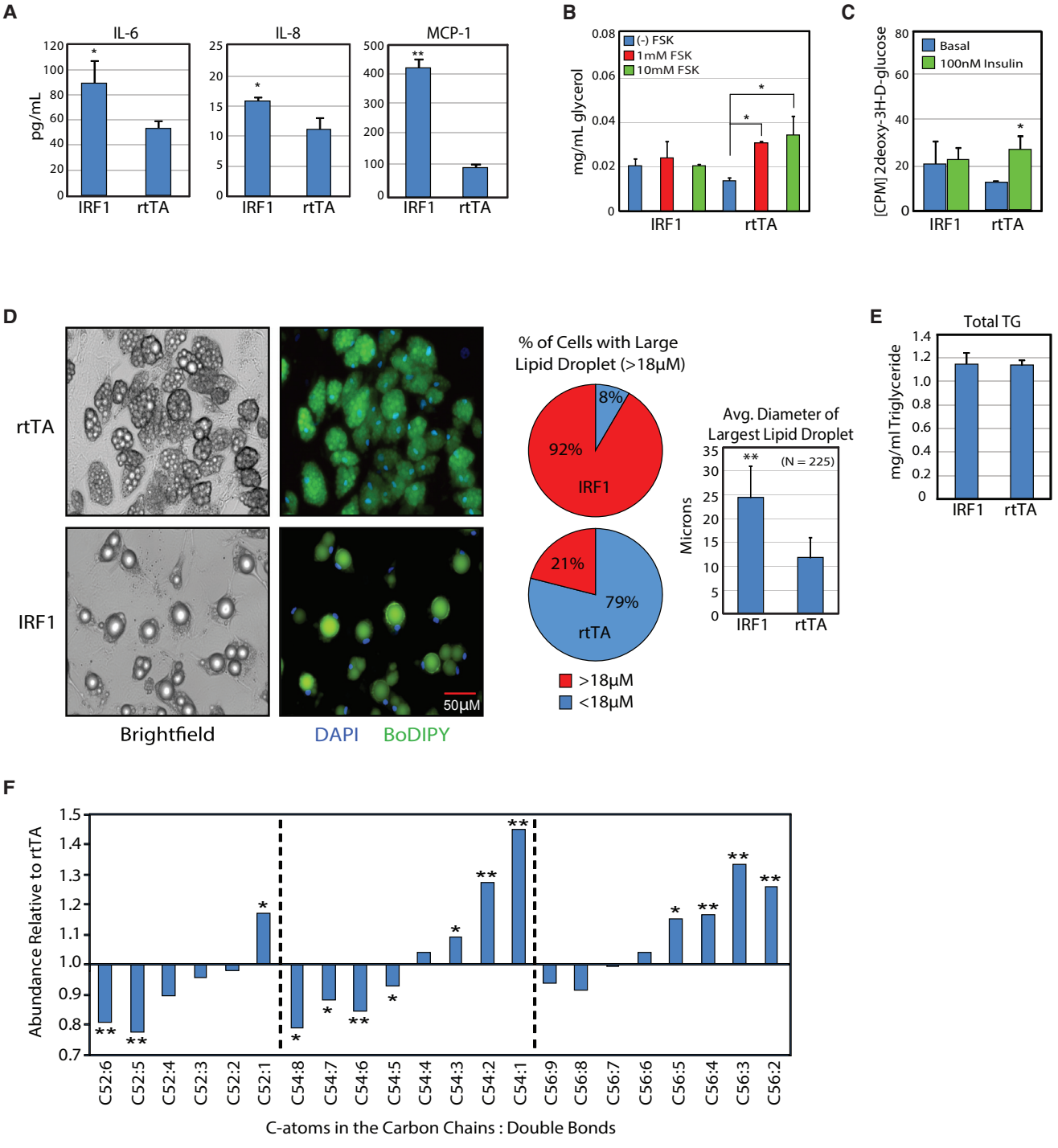

Figure 3. IRF1 Expression Impairs Adipocyte Metabolism and Affects Lipid Composition

(A) Multiplex ELISA assay was utilized to measure cytokines secreted into medium by IRF1 adipocytes compared with control adipocytes.

(B) Glycerol release into the medium in response to forskolin (FSK)-activated lipolysis was measured in IRF1 and rtTA adipocytes.

(C) Radiolabeled glucose uptake was measured in response to insulin.

(D) After 5 days of IRF1 expression, IRF1 adipocytes become unilocular. Lipid droplet size was measured after staining with the lipid dye BoDIPY (green) and the nuclear dye DAPI (blue). CPM, counts per minute.

(legend continued on next page)

(TG) content in IRF1 adipocytes is similar to that of ASC adipocytes, indicating no lipid uptake or synthesis phenotype (Figure 3E). These data suggest that IRF1 has a specific effect on lipid droplet coalescence. Next we used tandem mass spectroscopy to assess lipid composition. We found that intracellular TGs in IRF1 adipocytes exhibit a greater degree of saturation, with fewer double bonds ($p = 7 \times 10^{-6}$) and longer carbon chains ($p = 8 \times 10^{-6}$) (Figures 3F and S2F).

IRF1 Expression in Adipose Leads to Localized Inflammation In Vivo

IRF1-adipocyte phenotypes in vitro are consistent with those reported for inflamed primary adipose tissue; hence, we tested whether IRF1 also contributes to adipose inflammation in vivo. We transfected the adipogenic mouse cell line 3T3-F442A with a human *IRF1* (*hIRF1*) overexpression construct or control (Figure S3A). These cells were injected subcutaneously onto the flanks of nude mice. After 6 weeks of engraftment, ectopic fat pads were excised and assayed for inflammatory phenotypes (Figure 4A). We observed a significant increase in the number of macrophages localizing to implants expressing *IRF1* compared with control implants or autologous white adipose tissue (WAT) (Figures 4B, 3C, S3B, and S3C). IRF1 implants exhibited increased expression of MHC class II and MCP-1 compared with autologous WAT, as well as an increase in the macrophage-specific gene *F4/80*, in line with the immunostaining shown above (Figure 4D). Inexplicably, we did find noticeable differences in gene expression between autologous WAT of hIRF1 and rtTA (reverse tetracycline-controlled transactivator) mice despite using biological triplicates. While this is worrying, there is consistency with the staining data. Altogether these data are consistent with both the transcriptional analysis of primary adipocytes and in vitro assays performed in ASC adipocytes, and imply that *IRF1* contributes to adipose inflammation.

DISCUSSION

The mechanistic underpinnings of obesity's contribution to chronic adipose inflammation are poorly understood. Few transcriptional regulators have been identified that activate adipose inflammatory cascades in vivo. Progress is impeded by the lack of direct experimentation on primary adipocytes and reliance on in vitro systems that cannot recapitulate obesity, endocrine regulation, and immune system interactions. However, previous studies have implicated the major inflammatory transcription factors nuclear factor κB and activator protein 1 as possible mediators of adipose inflammation associated with obesity, but the mechanism for activation is unclear (Suganami et al., 2007; Osborn and Olefsky, 2012). This study found several inflammatory mediators differentially expressed in primary versus differentiated adipocytes, most notably *IRF1*. This result was verified in an independent dataset showing an increase of *IRF1* in obese individuals when compared with lean individuals. *IRF1* has been identified as a transcriptional activator of type I interferon gene activation in response to viral infection (Harada et al., 1989). Additionally it has been observed that *IRF4* represses early stages of adipogenesis (Eguchi et al., 2008) and modulates adipocyte lipid handling in vitro (Eguchi et al., 2011), suggesting a significant role for IRFs in adipose biology. However, there has been no study of *IRF1* in human adipocytes. Expression of *IRF1* in ASC adipocytes is sufficient to activate genes in the interferon response and inflammation pathways. Despite few transcriptional changes, *IRF1* overexpression leads to phenotypes associated with metabolic disease, including insulin resistance and attenuated lipolysis. Further supporting its role in adipose inflammation, expression of *IRF1* in 3T3-derived mouse adipose in vivo increases macrophage infiltration. We also demonstrate elevated MCP-1, which leads to inflammation and is associated with obesity, insulin resistance, and altered adipocyte metabolism (Kanda et al., 2006; Kim et al., 2006).

Lipidomic profiling of human subjects has revealed that the level of circulating saturated TGs is strongly correlated with insulin resistance and is a predictor of T2DM development (Rhee et al., 2011; Würtz et al., 2012). One striking phenotype of IRF adipocytes is the change in length and saturation level of TGs. The finding that expression of an immunoregulatory transcription factor leads to changes in composition of lipid droplet TGs is surprising. This finding in conjunction with our lipidomics data suggests that inflammation triggers production of more highly saturated fatty acids, in turn driving ER stress and further inflammation in a feedback loop (Wang et al., 2006). IRF1 adipocytes also acquire a unilocular lipid droplet, characteristic of primary adipocytes but absent in all in vitro models. Longer-chain, saturated TGs in IRF1 adipocytes could increase hydrophobicity of the intracellular lipids, potentiating the observed coalescence of lipids into a single large droplet.

(E) Total intracellular triglycerides (TG) were measured in IRF1 and rtTA adipocytes.
(F) Tandem mass spectrometric profiles of triglyceride composition for both IRF1 and rtTA adipocytes.
Error bars represent SD, experiments were performed in biological triplicates, and statistically significant p values are denoted by asterisks (*$p \leq 0.05$, **$p \leq 0.005$). n = 3 for each experiment.

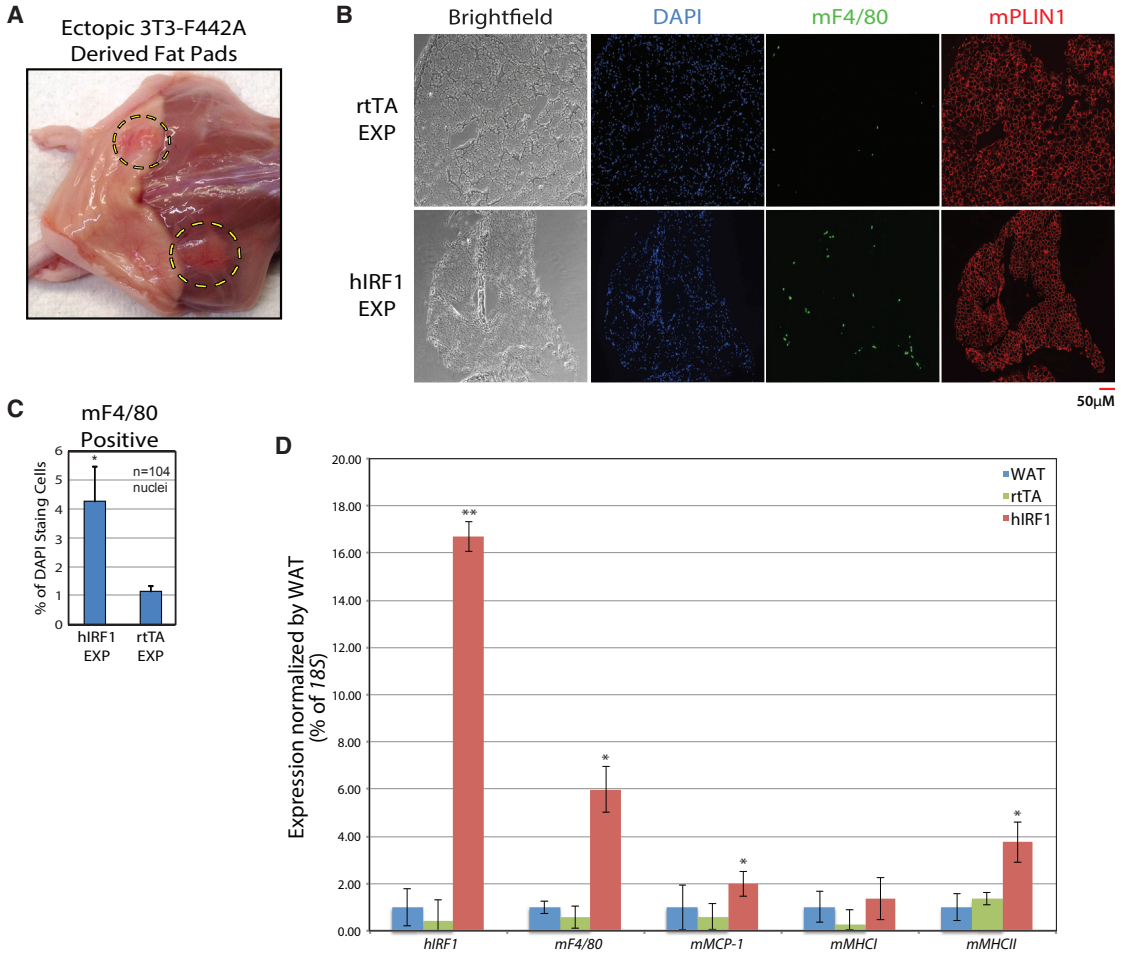

Figure 4. IRF1 Leads to Increased Inflammation In Vivo

(A) 3T3-F442A cells were transduced with either rtTA alone, or human IRF1 (hIRF1) containing lentiviral particles, and were injected into 6-week-old nude mice (n = 4). Six weeks after injection, ectopic subcutaneous fat pads (dashed circles) were excised.

(B) Ectopic fat explants (EXP) were stained with DAPI (blue) and probed with α-F4/80 (green) and α-PLIN1 (red).

(C) F4/80-positive cells were counted relative to DAPI staining foci in hIRF1 explants versus rtTA explants and autologous WAT (see Figure S3C). A minimum of 10^4 DAPI foci were counted for each experiment.

(D) qPCR was used to assess expression of hIRF1 and inflammation-associated mouse genes in both explants and autologous WAT (n = 3). Error bars represent SD, experiments were performed in biological triplicates, and statistically significant p values are denoted by asterisks (*$p \leq 0.05$, **$p \leq 0.005$).

Our data suggest that *IRF1* expression in human adipocytes contributes to adipose inflammation and insulin resistance.

EXPERIMENTAL PROCEDURES

Primary Adipocyte Isolation and ASC Cell Culture/Differentiation

Primary human adipocytes were obtained from discarded adipose tissue from two female elective abdominoplasty patients. Whole adipose was chopped up and digested with Liberase Blendzyme (Roche) for 1 hr at 37°C, forced through a 250-μm filter, and centrifuged. The floating adipocyte fraction was washed with PBS and re-collected. The stromovascular cell pellet was washed twice with PBS and plated onto gelatin-coated plates in ASC growth medium (DMEM, 10% fetal bovine serum [FBS], 1% penicillin-streptomycin, and 2.5 ng/mL basic fibroblast growth factor [Aldevron]). ASCs were brought to homogeneity by passaging and when ~95% confluent, adipocyte medium (DMEM, 10% FBS, 1% penicillin-streptomycin, 0.1 μM dexamethasone, 10 μg/mL insulin, 0.5 μM rosiglitazone, 250 μM 3-isobutyl-1-methylxanthine [IBMX]) was added for 5 days. On day 6, ASCs were switched to adipocyte medium without IBMX for 14 additional days.

RNA Extraction/qRT-PCR/Transcriptional Profiling

Total RNA from all cell preparations was extracted using TRIzol (Invitrogen). RNA quality was determined using an RNA nanochip

on a Bioanalyzer (Agilent Technologies). RNA was converted to cDNA using the Superscript First-Strand III kit (Invitrogen) and qRT-PCR was carried out using a Realplex Mastercycler (Eppendorf) with Quantifast-SYBR Green Mastermix (Qiagen). Primer sets are listed in supplemental Experimental Procedures.

RNA samples were processed by Asuragen and microarray analysis was performed on the Affymetrix Human Genome U133 Plus 2.0 Array. Arrays were hybridized overnight at 50°C, washed, stained, and scanned on a GeneChip Scanner 3000. Microarray data was analyzed using R/Bioconductor (http://www.bioconductor.org). Raw data were normalized by robust multi-array averaging (Bolstad et al., 2003) using a custom Chip Description File from the Michigan Microarray Lab (http://brainarray.mbni.med.umich.edu, version 13). Primary adipocyte RNA is from Zenbio, cat. #RNAmi-Q10-1, RNAmi-Q10-2, and RNA-Q10-3. GEO data were taken from Lee et al. (2005), dataset record GEO: GDS3602.

Microarray Gene and Sample Clustering

To select a minimally biased set of genes for hierarchical clustering, we used the R package limma (Smyth, 2005) to test for differential expression across all ten pairwise comparisons between biologically distinct samples: primary adipocytes (59 and 41 years of age), ASCs (59 years), ASC adipocytes (59 years), and the pelleted SVF from disassociated adipose tissue (59 years). Hierarchical clustering was performed on the 2,489 probe sets with five or more significantly different pairwise comparisons (FDR = 0.001). The hmap function in the seriation R package (Hahsler et al., 2008) was used to generate the heatmap.

Production of Inducible Transgenes/Lentivirus Transduction

Doxycycline-inducible lentiviral Gateway (Invitrogen) vector containing *IRF1* was constructed by PCR amplification from verified cDNA clones (GenBank: NM_002198) (GeneCopoeia), and standard TOPO cloning (Invitrogen) techniques were used to generate entry clones. The *IRF1* construct was transduced via calcium chloride transfection into HEK293T cells as previously described (al Yacoub et al., 2007). Media containing viral supernatant was collected, filtered, and used to infect ASC adipocytes. Infection efficiency was measured as compared by co-infection with a GFP lentiviral construct. Expression of IRF1 was induced by addition of doxycycline (1 μg/mL final) to the adipogenic medium.

ChIP

ASC adipocytes were crosslinked in 1% formaldehyde and quenched with glycine (200 mM final). Cells were washed several times in PBS. ChIP-qPCR was performed with an antibody against IRF1 (Santa Cruz Biotechnology, sc-497) as previously described (Camahort et al., 2007). All ChIPs were graphed as percentage of total chromatin input. qPCR was performed as described above.

Protein Normalization

Protein concentration used to normalize other assays was measured using the Bradford protein assay (Bio-Rad).

Metabolic Assays

For glucose uptake, after 5 days of IRF1 expression ASC adipocytes were serum starved in low-glucose DMEM containing 0.2% BSA overnight. Cells were incubated in KRH buffer (120 mM NaCl, 5 mM KCl, 1 mM $MgSO_4$, 0.3 mM $CaCl_2$ and 10 mM HEPES [pH 7.4]) in the presence or absence of 100 nM insulin for 30 min at 37°C. Non-specific uptake was measured in the presence of 10 μM cytochalasin B. Glucose uptake was measured by incubating cells with 0.5 $\mu Ci/mL^{-1}$ 2-deoxy-D-[^{3}H]glucose (Perkin-Elmer) for 5 min at 37°C.

For glycerol release, after 5 days of *IRF1* expression ASC-adipocyte cells were starved in DMEM with 1% FBS for 1 hr and then incubated in Hank's balanced salt solution with 2% fatty acid-free BSA with forskolin for 1 hr (0 μM, 1 μM, and 10 μM). The incubation medium was collected for glycerol measurement using a colorimetric assay kit (Sigma).

All assays were performed in biological triplicates and normalized to protein.

Multiplex ELISA Assay

Medium was collected 5 days after IRF1 expression and ELISA was performed on a Luminex 200 analyzer using the Human Adipocyte Multiplex Panel (Millipore, HADCYMAG-61K) as per manufacturer's instructions. The assay was performed in biological triplicate and normalized to protein.

Triglyceride Analysis/Lipidomics

Total TG levels were measured using a colorimetric assay kit (Cayman Chemicals). Protein concentration was used to normalize intracellular TG content. For lipidomics, after 5 days of transgene expression ASC adipocytes were washed with fresh medium. Ice-cold isopropanol was added, and cells were scraped and collected into cold tubes. Extracts were incubated for 1 hr at 4°C, than vortexed and centrifuged at 2,300 × *g* for 10 min. The supernatant was used for mass spectroscopic analysis. All data were acquired using a Sciex 4000 QTRAP mass spectrometer as previously described (Rhee et al., 2011). MultiQuant software (version 1.1; Applied Biosystems/Sciex) was used for automated peak integration, and peaks were manually reviewed for quality of integration. Internal standard peak areas were monitored for quality control and used to normalize analyte peak areas.

For the transduced ASCs we averaged six replicates for metabolite abundance of 44 TG species and computed an abundance ratio of the two (IRF1/rtTA). We built a regression model, predicting the abundance ratio using number of double bonds and total number of carbon atoms as variables as well as an interaction term to assess whether the relationship with number of double bonds varies with carbon number. Statistical significance of regression coefficients was assessed using the F test.

Transplantation

Differentiated 3T3-F442A preadipocytes were transduced with hIRF-1 or rtTA lentivirus at day 7 and injected subcutaneously on the backs of 6-week-old female NCr nude mice (n = 4, Taconic). The cells developed into mature adipocytes over the next 6 weeks. Mice were euthanized to harvest fat pads which were fixed,

embedded in paraffin, and stained after sectioning. Harvard University Animal Care and Use Committee approved all animal procedures.

Immunostaining

The following antibodies and dilutions were used: α-CEBPA 1:100 (Santa Cruz, sc-61), α-PLIN1 1:200 (Sigma, P1873), and α-F4/80 1:200 (eBioscience, 14-4801-81). Lipid droplets were stained using BoDIPY neutral lipid dye (Thermo Fisher, D-3922), cell membranes using LavaCell dye (Active Motif, 15004), and cell nuclei with DAPI. Images were acquired using a Nikon Eclipse Ti-S microscope. Both NIS-Elements and ImageJ software packages were used for image analysis.

ACCESSION NUMBERS

All microarray data were deposited in the GEO under GEO: GSE96062.

SUPPLEMENTAL INFORMATION

Supplemental Information includes Supplemental Experimental Procedures, three figures, and five tables and can be found with this article online at http://dx.doi.org/10.1016/j.stemcr.2017.03.014.

AUTHOR CONTRIBUTIONS

M.F. and R.C. performed the research and wrote the manuscript. Y.-K.L. performed the research with support of F.X. R.E.G. and E.P.R. performed the lipidomics. R.C.D. carried out the bioinformatics analysis. C.A.C. designed the study, supported the finance, and approved the final manuscript.

ACKNOWLEDGMENTS

We thank Greg Mower, and former and current members of the C.A.C. laboratory for technical assistance and discussion. We would also like to thank Alexa Nicholls of the Division of Plastic & Reconstructive Surgery at Massachusetts General Hospital for coordinating acquisition of human adipose tissue. R.C.D. acknowledges support from NIH/NHLBI K08 HL098361.

Received: September 14, 2016
Revised: March 10, 2017
Accepted: March 12, 2017
Published: April 13, 2017

REFERENCES

ADA. (2012). American Diabetes Association—standards of medical care in diabetes. Diabetes Care *35*, S11–S63.

al Yacoub, N., Romanowska, M., Haritonova, N., and Foerster, J. (2007). Optimized production and concentration of lentiviral vectors containing large inserts. J. Gene Med. *9*, 579–584.

Bolstad, B.M., Irizarry, R.A., Astrand, M., and Speed, T.P. (2003). A comparison of normalization methods for high density oligonucleotide array data based on variance and bias. Bioinformatics *19*, 185–193.

Camahort, R., Li, B., Florens, L., Swanson, S.K., Washburn, M.P., and Gerton, J.L. (2007). Scm3 is essential to recruit the histone h3 variant cse4 to centromeres and to maintain a functional kinetochore. Mol. Cell *26*, 853–865.

Eguchi, J., Yan, Q.W., Schones, D.E., Kamal, M., Hsu, C.H., Zhang, M.Q., Crawford, G.E., and Rosen, E.D. (2008). Interferon regulatory factors are transcriptional regulators of adipogenesis. Cell Metab. *7*, 86–94.

Eguchi, J., Wang, X., Yu, S., Kershaw, E.E., Chiu, P.C., Dushay, J., Estall, J.L., Klein, U., Maratos-Flier, E., and Rosen, E.D. (2011). Transcriptional control of adipose lipid handling by IRF4. Cell Metab. *13*, 249–259.

Gregor, M.F., and Hotamisligil, G.S. (2011). Inflammatory mechanisms in obesity. Annu. Rev. Immunol. *29*, 415–445.

Hahsler, M., Hornik, K., and Buchta, C. (2008). Getting things in order: an introduction to the R package seriation. J. Stat. Software *25*, 1–34.

Harada, H., Fujita, T., Miyamoto, M., Kimura, Y., Maruyama, M., Furia, A., Miyata, T., and Taniguchi, T. (1989). Structurally similar but functionally distinct factors, IRF-1 and IRF-2, bind to the same regulatory elements of IFN and IFN-inducible genes. Cell *58*, 729–739.

Kanda, H., Tateya, S., Tamori, Y., Kotani, K., Hiasa, K., Kitazawa, R., Kitazawa, S., Miyachi, H., Maeda, S., Egashira, K., et al. (2006). MCP-1 contributes to macrophage infiltration into adipose tissue, insulin resistance, and hepatic steatosis in obesity. J. Clin. Invest. *116*, 1494–1505.

Kim, C.S., Park, H.S., Kawada, T., Kim, J.H., Lim, D., Hubbard, N.E., Kwon, B.S., Erickson, K.L., and Yu, R. (2006). Circulating levels of MCP-1 and IL-8 are elevated in human obese subjects and associated with obesity-related parameters. Int. J. Obes. *30*, 1347–1355.

Lee, Y.H., Nair, S., Rousseau, E., Allison, D.B., Page, G.P., Tataranni, P.A., Bogardus, C., and Permana, P.A. (2005). Microarray profiling of isolated abdominal subcutaneous adipocytes from obese vs non-obese Pima Indians: increased expression of inflammation-related genes. Diabetologia *48*, 1776–1783. http://dx.doi.org/10.1007/s00125-005-1867-3.

McGillicuddy, F.C., Chiquoine, E.H., Hinkle, C.C., Kim, R.J., Shah, R., Roche, H.M., Smyth, E.M., and Reilly, M.P. (2009). Interferon γ attenuates insulin signaling, lipid storage, and differentiation in human adipocytes via activation of the JAK/STAT pathway. J. Biol. Chem. *284*, 31936–31944.

Ogden, C.L., Carroll, M.E., Kit, B.K., and Flegal, K.M. (2012). Prevalence of obesity in the United States, 2009-2010. NCHS Data Brief, 1–8.

Osborn, O., and Olefsky, J.M. (2012). The cellular and signaling networks linking the immune system and metabolism in disease. Nat. Med. *18*, 363–374.

Rhee, E.P., Cheng, S., Larson, M.G., Walford, G.A., Lewis, G.D., McCabe, E., Yang, E., Farrell, L., Fox, C.S., O'Donnell, C.J., et al. (2011). Lipid profiling identifies a triacylglycerol signature of insulin resistance and improves diabetes prediction in humans. J. Clin. Invest. *121*, 1402–1411.

Samarajiwa, S.A., Forster, S., Auchettl, K., and Hertzog, P.J. (2009). INTERFEROME: the database of interferon regulated genes. Nucleic Acids Res. *37*, D852–D857.

Smyth, G.K. (2005). Limma: linear models for microarray data. In Bioinformatics and Computational Biology Solutions Using R and Bioconductor, R. Gentlemen, V. Carey, W. Huber, R. Irizarry, and S. Dudoit, eds. (Springer), pp. 397–420.

Suganami, T., Tanimoto-Koyama, K., Nishida, J., Itoh, M., Yuan, X., Mizuarai, S., Kotani, H., Yamaoka, S., Miyake, K., Aoe, S., et al. (2007). Role of the toll-like receptor 4/NF-κB pathway in saturated fatty acid-induced inflammatory changes in the interaction between adipocytes and macrophages. Arterioscler. Thromb. Vasc. Biol. *27*, 84–91.

Urs, S., Smith, C., Campbell, B., Saxton, A.M., Taylor, J., Zhang, B., Snoddy, J., Jones Voy, B., and Moustaid-Moussa, N. (2004). Gene expression profiling in human preadipocytes and adipocytes by microarray analysis. J. Nutr. *134*, 762–770.

Wang, D., Wei, Y., and Pagliassotti, M.J. (2006). Saturated fatty acids promote endoplasmic reticulum stress and liver injury in rats with hepatic steatosis. Endocrinology *147*, 943–951.

Würtz, P., Mäkinen, V.-P., Soininen, P., Kangas, A.J., Tukiainen, T., Kettunen, J., Savolainen, M.J., Tammelin, T., Viikari, J.S., Rönnemaa, T., et al. (2012). Metabolic signatures of insulin resistance in 7,098 young adults. Diabetes *61*, 1372–1380.

Stem Cell Reports, Volume *8*

Supplemental Information

Activation of IRF1 in Human Adipocytes Leads to Phenotypes Associated with Metabolic Disease

Max Friesen, Raymond Camahort, Youn-Kyoung Lee, Fang Xia, Robert E. Gerszten, Eugene P. Rhee, Rahul C. Deo, and Chad A. Cowan

Figure S1, Adipocyte identity validation. Related to Figure 1.

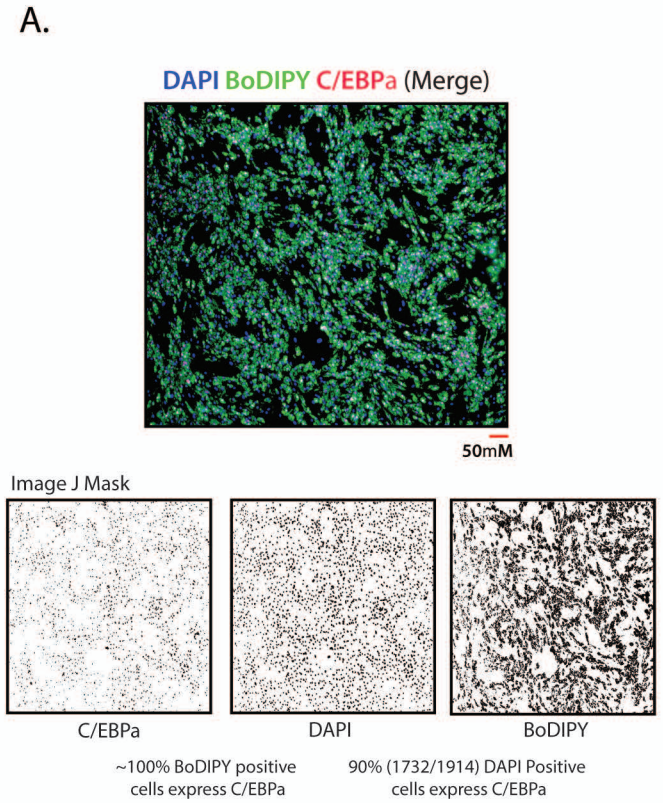

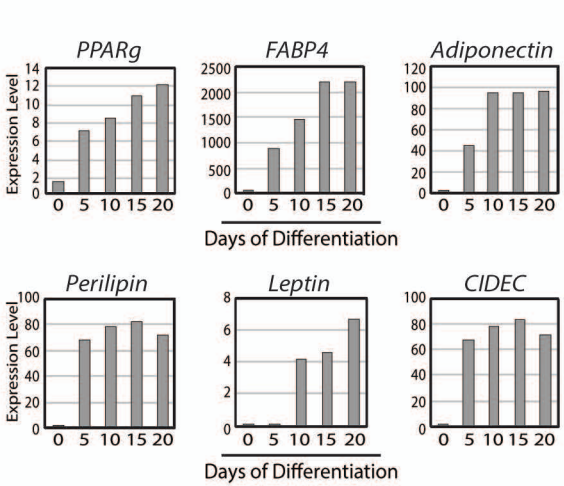

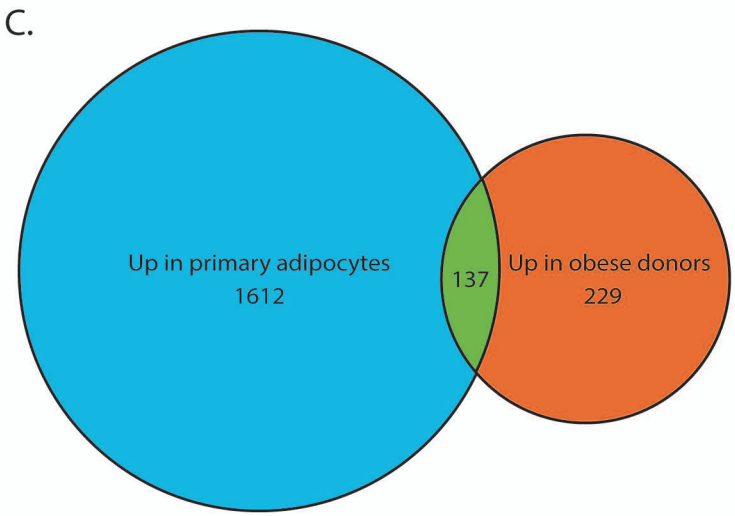

Figure S2, IRF1 overexpression. Related to Figure 2 & 3.

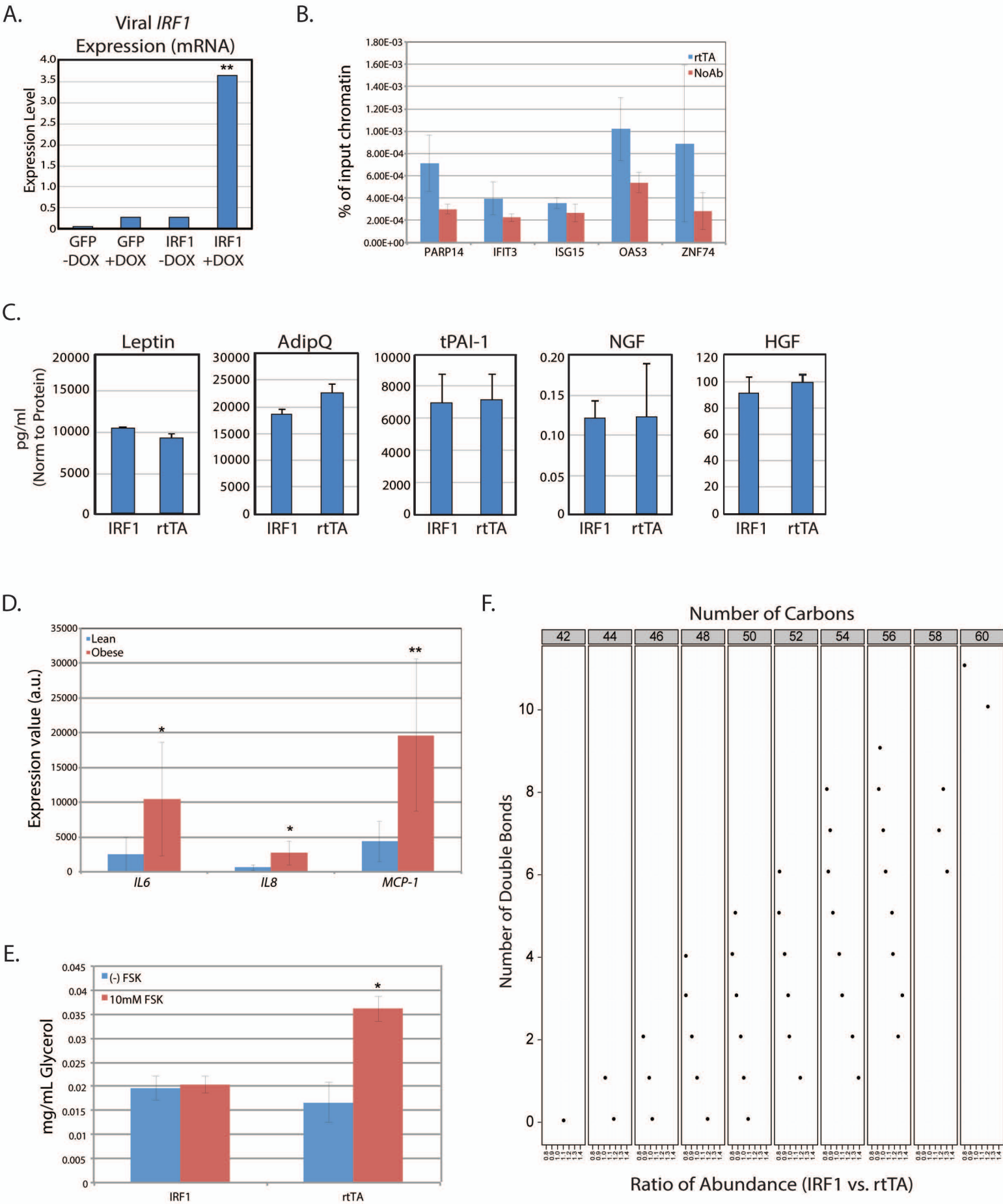

Figure S3, *In vivo* IRF1 expression. Related to Figure 4.

A.

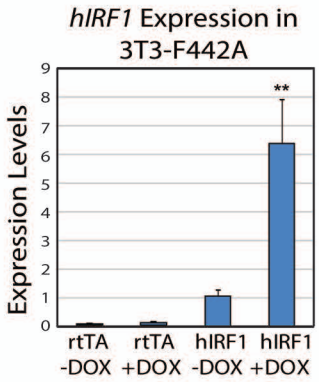

B.

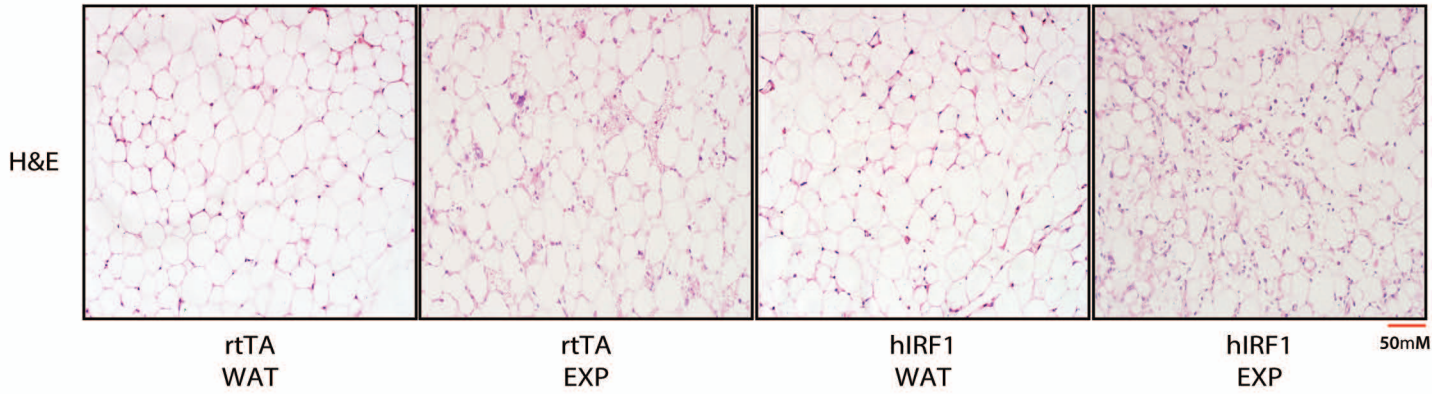

C.

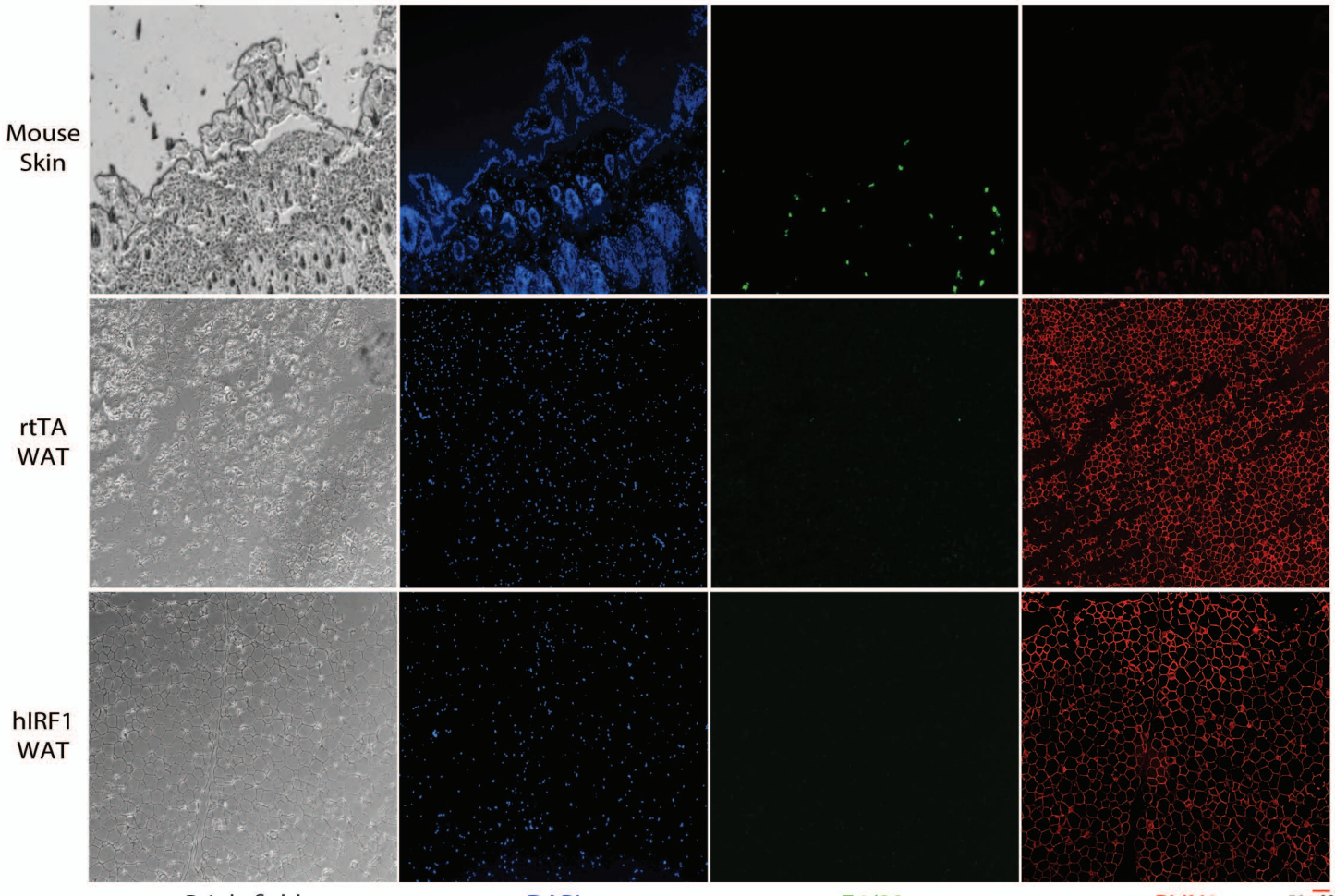

Supplemental Figure Legends

Figure S1. A) ASC-adipocytes were co-stained with BoDIPY (green), DAPI (blue), and anti-C/EBPα (red) to assess differentiation efficiency. An Image J binary mask was used to count stained foci. B) RT-qPCR was used to quantify expression of adipogenic genes during a timecourse of ASC-adipocyte differentiation. "Day 0" represents undifferentiated ASCs. C) Venn diagram of genes higher expressed in primary adipocytes versus ASC-adipocytes overlapping with genes higher expressed in obese versus lean individuals.

Figure S2. Error bars represent +/- standard deviation of biological triplicates and statistically significant p-values are denoted by an asterisk (*≤0.05, **≤0.005). A) RT-qPCR was used to test expression of the inducible IRF1 transgene in ASC-adipocytes, in both the presence and absence of doxycycline (+/- DOX). ASC-adipocyte transfection with a DOX-inducible GFP transgene serves as a negative control. B) ChIP/qPCR was performed for IRF1 in rtTA control cells without IRF1 expression at putative binding sites (H3K4me1 bound IRF1 motif) (*PARP14, IFIT3, ISG15*). *OAS3* and *ZNF74* represent a negative control site where IRF1 is not predicted to bind. Signals are expressed as percentage of total chromatin input. C) A multiplex ELISA assay was utilized to measure adipokines and cytokines in secreted into culture media from adipocytes expressing IRF1. D) Expression of IL6, IL8 and MCP-1 in obese and lean individuals' adipocytes from the GEO dataset, related to figure 3A. E) Glycerol release into the media in response to forskolin (FSK) activated lipolysis was measured in IRF1- and rtTA-adipocytes. Two separate biological triplicates were averaged and plotted. Replication of and related to figure 3B. F) A plot of abundance ratio against number of double bonds for each total of carbon atoms for triglycerides in IRF-adipocytes vs. control (rtTA).

Figure S3. A) RT-qPCR was used to assay for doxycycline (DOX)-inducible expression of hIRF1 in 3T3-F442A cells. B) rtTA only or IRF1-expressing 3T3-F442A cells from were injected into 6-week old nude mice. 6 weeks post-injection, exogenous fat explants (EXP) and control autologous white adipose tissue (WAT) were harvested and stained with hemotoxylin and eosin (H&E). C) Autologous WAT and skin (positive control for macrophage localization) were harvested, probed with anti-F4/80 (green) to assess macrophage infiltration, α-PLIN1 (red) to verify adipocyte identity, and stained with DAPI. Negligible numbers of macrophages are observed in control WAT.

Supplemental experimental procedures

Primer List

Expression Analysis

hMCP-1 exp For #1	CAG CCA GAT GCA ATC AAT GCC
hMCP-1 exp Rev #1	TGG AAT CCT GAA CCC ACT TCT
mf4/80 exp For #1	TTG TAC GTG CAA CTC AGG ACT
mf4/80 exp Rev #1	GAT CCC AGA GTG TTG ATG CAA
mMHCI F	GTGATCTCTGGCTGTGAAGT
mMHCI R	GTCTCCACAAGCTCCATGTC
mMHCII F	CAACCGTGACTATTCCTTCC
mMHCII R	CCACAGTCTCTGTCAGCTC
Viral IRF1 qPCR 1 For	TCT GAA GAA CAT GGA TGC CAC C
pDL38R (LentiViral 3'UTR) Rev	AGCAGCGTATCCACATAG
ADIPOQ For	GATGAAGTCCTGTCTTGGAAGG
ADIPOQ Rev	CAGCACTTAGAGATGGAGTTGG
FABP4 For	TCATGAAAGGCGTCACTTCC
FABP4 Rev	GCTTGCTAAATCAGGGAAAACA
PPARG2 For	GCAGGAGATCTACAAGGACTTG
PPARG2 Rev	CCCTCAGAATAGTGCAACTGG
Lep For	AAGGTTTGGTGTGTGGAGATG
Lep Rev	CTCCTGTCTCTTCTTTCTCTGC
PLIN1 For	CCCCCTGAAAAGATTGCTTCT
PLIN1 Rev	GGAACGCTGATGCTGTTTCTG
CIDEC For	AAGTCCCTTAGCCTTCTCTACC
CIDEC Rev	CCTTCCTCACGCTTCGATCC
HPRT For	TGACACTGGCAAAACAATGCA
HPRT Rev	GGTCCTTTTCACCAGCAAGCT

ChIP-qPCR

IFIT3 Prom ChIP-1 For	CTG AGG CAG GAG AAT CAC TT
IFIT3 Prom ChIP-1 Rev	TGA CTG TTG CTC TTT GAC CT
PARP 14 ChIP-1 For	GAT CTC TCT GCC TCC ACT CT
PARP 14 ChIP-1 Rev	GAT ATC AGG GGA TAG CCT TG
ISG15 ChIP For	CGC TTT GTG ACC AGA CCT CAC T
ISG15 ChIP Rev	ATT TTG AAG GCA TGG CCG G
IRS-1 ChIP For	TTTCTCCACCCGCCGAGATG
IRS-1 ChIP Rev	CAGCGATTCCCGAGGCAAAT